Radboud University Nijmegen

Theoretical High Energy Physics

Bachelor thesis

The High Energy Behaviour of the Higgs Potential

Author:
Jorn Biemans

Supervisor:
Dr. Wim Beenakker

July 23, 2013

Contents

1 Introduction and Research question

In the previous year the discovery of the Higgs boson was hailed as one of the greatest achievements that has been made in science. While its discovery is certainly important it doesn't solve all the problems that exist in the standard model. The standard model is the theory in which the electroweak and strong interactions of particle physics are unified. In fact with the discovery of the Higgs boson some new problems, that were previously purely theoretical, have revealed themselves. One of the problems can be found in the high energy behaviour of the Higgs potential. This problem is detailed in the article by J. Ellis, J.R. Espinosa, G.F. Giudice, A. Hoecker and A. Riotto called "The Probable Fate of the Standard Model" [7]. It concerns the evolution of the Higgs potential as a function of energy. For this evolution different scenarios are possible depending on the mass of the Higgs boson, since this mass was determined last year a prediction can be made about the evolution of the Higgs potential.

There are some theories beyond the standard model that solve these problems like supersymmetry. But currently no experimental evidence has been found for any of these theories. The goal of this thesis is to determine the influence of standard model[1] parameters upon the high energy behaviour. In the SM all parameters are included. But a simplified model of the SM is used, since the complete SM is a complex system in which the effects of individual parameters are difficult to determine. Furthermore, some constraints might be loosened to determine their effects upon the high energy behaviour. This brings us to the following research question:

Which parameters determine the high energy behaviour of the Higgs potential

To answer this question, some theoretical concepts need to be used. The most important ones are explained in the second chapter. These include the Higgs mechanism and renormalization. These concepts will be needed to analyse the effect that a high energy limit has on the simplified model that is being used. This is detailed in the third chapter. In the fourth chapter the conclusions of the research will be given and a short summary of possible implications will also be given.

In this thesis natural units ($c = 1$ and $\hbar = 1$) will be used.

[1] This will be abbreviated as SM in the rest of the thesis

2 Theoretical Background

2.1 Gauge Invariance

One of the properties that has a great impact on the description of a physical system is symmetry. When a system displays symmetry this means that a certain transformation has no effect on the theory. For example, if a system has translation symmetry it will stay the same even when shifted in spacetime. In the following paragraph a quick introduction will be given of a symmetry phenomenon known as gauge invariance.
There are two forms of symmetries: global and local ones.
A global one states that if this symmetry is applied uniformly in each postion of spacetime the physics won't change. To illustrate this let's consider a Lagrangian $\mathcal{L}$ that depends on a Dirac field ψ:

$$\mathcal{L} = i\bar{\psi}\gamma^{\mu}\partial_{\mu}\psi \tag{1}$$
$$\tag{2}$$

In this equation the repeared us of the spacetime index $\mu(0,...,3)$ implies a summation over that index. This is called the Einstein convention and states that an index that appears both as a lower index and as a upper index is summed over all possible values. This leaves γ^{μ}, ∂_{μ} and $\bar{\psi}$. Firstly ∂_{μ} is the derivative with the index denoting with respect to which spacetime coordinate the derivative is taken. Secondly γ^{μ} are a set of matrices known as the gamma matrices of Dirac. Finally, $\bar{\psi}$ is a shortened notation for $\psi^{\dagger}\gamma^{0}$ which is a specific combination of the hermitian conjugate of our Dirac field ψ and the gamma matrix γ^{0}.
Giving the field a global phase results in:

$$\begin{aligned} &\psi \longrightarrow \psi' = e^{iQ\alpha}\psi \\ &\mathcal{L}' = i\bar{\psi}'\gamma^{\mu}\partial_{\mu}\psi' = ie^{-iQ\alpha}\bar{\psi}\gamma^{\mu}\partial_{\mu}e^{iQ\alpha}\psi = i\bar{\psi}\gamma^{\mu}\partial_{\mu}\psi = \mathcal{L} \end{aligned} \tag{3}$$

Let's quickly introduce the new variables, α is a real phase and Q can be considered to be akin to a charge.
Since ψ and $\bar{\psi}$ differ by a complex conjugate, the Lagrangian is gauge invariant under a global phase transformation (gauge transformation).

The second type of symmetry is a local symmetry. The difference with the global one is that the transformation may now depend on the position in spacetime. Thus in this example the phase becomes $\alpha(x)$ which depends on the position. Clearly this will give a great difference with the global phase. The derivative will act on the phase, now giving extra terms:

$$\partial_{\mu}\psi \longrightarrow \partial_{\mu}\psi' = e^{iQ\alpha(x)}\partial_{\mu}\psi + iQe^{iQ\alpha(x)}\psi(\partial_{\mu}\alpha(x)) \tag{4}$$

Note that the second term would be zero in the global case. But in this case the Lagrangian is no longer invariant under this transformation:

$$\begin{aligned} &\mathcal{L}' = ie^{-iQ\alpha(x)}\bar{\psi}\gamma^{\mu}\partial_{\mu}(e^{iQ\alpha(x)}\psi) \\ &\mathcal{L}' = ie^{-iQ\alpha(x)}\bar{\psi}\gamma^{\mu}\left(e^{iQ\alpha(x)}\partial_{\mu}\psi + \psi\partial_{\mu}\left(e^{iQ\alpha(x)}\right)\right) \end{aligned} \tag{5}$$

Assume now that similar to the global gauge invariance, the Lagrangian happens to be also locally gauge invariant.
To achieve this, let's introduce a new derivative D_μ in such a way that:

$$D_\mu \psi \longrightarrow D'_\mu \psi' = e^{iQ\alpha(x)} D_\mu \psi \tag{6}$$

This can be realized by defining D_μ as

$$D_\mu = \partial_\mu + igQA_\mu \tag{7}$$

In this definition g is a coupling constant (interaction strength) and A_μ is a new vector field that Lorentz transforms like ∂_μ. Furthermore A_μ has the property that its gauge transformation will cancel the extra term that was found in equation (5):

$$A_\mu \longrightarrow A'_\mu = A_\mu - \frac{1}{g}\partial_\mu \alpha(x) \tag{8}$$

Thus by replacing all ∂_μ by D_μ, it's ensured that $\mathcal{L}$ is locally invariant under this gauge transformation [10].
So what are the consequences of assuming a local gauge invariance? We introduced a new vector field which had an interaction strength that is determined by g. This means that this vector field can interact with our Dirac field, this wasn't the case earlier. Thus by assuming a local gauge invariance we can introduce interactions between Dirac fields (particles) transmitted by vector fields. This turns out to be a good method to describe most interaction in physics, thus the postulate of local gauge invariance is an important tool in high-energy physics.

2.2 The Higgs Mechanism

Consider a system with a massless complex scalar field ϕ' in a potential $V(\phi')$ similar to the one created by the Higgs field. The Lagrangian of this system will be

$$\mathcal{L} = (\partial_\mu \phi')^\dagger (\partial^\mu \phi') - V(\phi') \tag{9}$$

$$V(\phi') = -\mu^2 \phi'^\dagger \phi' + \lambda(\phi'^\dagger \phi')^2 \tag{10}$$

With μ and λ real and positive parameters. When taking a closer look at the potential $V(\phi')$, it reveals that its minimum isn't at the origin $\phi' = 0$. It's shifted and that presents a problem. If the current field ϕ' is used to define a groundstate, we don't get the desired result. We want the groundstate to have an expectation value of 0, but with ϕ' this isn't the case, since its value at the minimum of the potential isn't 0. This also means that the particle interpretation isn't correct, only around a minimum can we correctly look at the particle interpretation. The field must be shifted in order to find the correct particle interpretation.
In figure 1 the potential has been plotted. We define the distance between the origin and the minima as $\frac{v}{\sqrt{2}}$. This value gives the expectation value for the groundstate and can be derived to be

$$v^2 = \frac{\mu^2}{\lambda} \tag{11}$$

This gives a ring of possible groundstates in the complex plane spanned by ϕ'. Since only one can be the real groundstate, the symmetry of our system has to be broken. This is called *spontaneuos symmetry breaking*, nature chooses one solution for the groundstate and breaks the symmetry.

The field can now be shifted, since the minimum of the potential is known. Since ϕ' is a complex field it can be decomposed in two parts. We choose the real part to be shifted giving us:

$$\phi' = \frac{1}{\sqrt{2}}(\phi'_1 + i\phi'_2)$$

$$\phi_1 = \phi'_1 - v \qquad\qquad \phi_2 = \phi'_2$$

From this shift the old ϕ' can be written into a new form consisting of the transformed components:

$$\phi' = \frac{1}{\sqrt{2}}\left(\phi_1 + v + i\phi_2\right) \tag{12}$$

By inserting this shift into equation (10), a transformed potential can be determined:

$$\begin{aligned}
V(\phi') &= -\frac{1}{2}\mu^2(\phi_1 + v - i\phi_2)(\phi_1 + v + i\phi_2) + \frac{1}{4}\lambda((\phi_1 + v - i\phi_2)(\phi_1 + v + i\phi_2))^2 \\
&= -\frac{\mu^2}{2}((\phi_1 + v)^2 + \phi_2^2) + \frac{\lambda}{4}((\phi_1 + v)^4 + 2(\phi_1 + v)^2\phi_2^2 + \phi_2^4) \\
&= \mu^2\phi_1^2 - \frac{\mu^2 v^2}{4} + \frac{\lambda}{4}(4v\phi^3 + 4v\phi_1\phi_2^2 + (\phi_1^2 + \phi_2^2)^2) \\
&= \mu^2\phi_1^2 - \frac{\mu^2 v^2}{4} + \text{interactions}
\end{aligned} \tag{13}$$

The number of fields is important to determine what the various terms in the potential represent. A term with 2 fields like ϕ_1^2 is called a mass term. This is a byproduct of the shift. The mass term has a negative sign in the Lagrangian. However, our old field had the term $-\mu^2\phi'\phi'^{\dagger}$, which would have a positive sign in the Lagrangian. Now we have a new term with ϕ_1 which is positive in the potential and thus negative in the Lagrangian, just as we expect of a mass term. The shift of the old field has given us a correct mass term.
All terms with more fields are called interactions and are left out in the final formula. The last term is a constant term that doesn't depend on any fields. This can be considered to be some kind of vacuum energy
Let's return to equation (13), it can be seen that a mass term has appeared for the field ϕ_1, while the field ϕ_2 remains massless. The massless particle represents the groundstate symmetry still present in the potential. But a gauge transformation can be performed[2] to get rid of the massless field. When this is done then only the massive particle remains. This process is called the Higgs mechanism [3].

[2]This will be done in section 3.2.

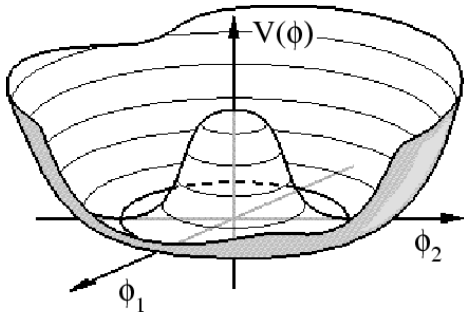

Figure 1: The Higgs potential [8]

2.3 High Energy Behaviour

One of the goals of a theory is to make predictions at energy scales that haven't been probed with experiments. A way to do this is to look at the high energy behaviour of a theory. This can be done by looking at the evolution of parameters as a function of energy. Therefore let's look at a simple ϕ^4-theory for which the Lagrangian looks like:

$$\mathcal{L} = \frac{1}{2}\partial_\mu\phi\partial^\mu\phi - \frac{\lambda}{4!}\phi^4 \tag{14}$$

In this Lagrangian ϕ is a real scalar field and λ is the coupling constant of the quartic interaction. To study the high energy behaviour we can study the parameter λ and how it depends on energy.
How should this be done? Firstly, Quantum Field Theory[3] is based on perturbation theory. This means that we can calculate the probability of a process by using pieces of perturbation theory.
But before one can calculate a probability, a process should be specified. The simplest process is scalar boson scattering, which can be represented by a Feynman diagram that looks like the diagram depicted in figure 2. Now, how should

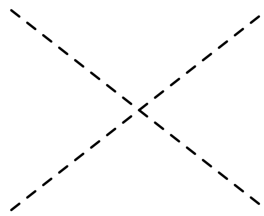

Figure 2: Lowest order Feynman diagram for scalar boson scattering

we interpret this diagram. Firstly the time axis is chosen horizontally from left to right. Furthermore there are different representations for different types of particles. The particles in figure 2 are scalar bosons. Thus the diagram should be read as two scalar bosons interacting and scattering to two scalar bosons.

[3] QFT

The probability interpretation of a scattering process, is represented by its matrix element M. The value of $|M|^2$ is directly linked to the chance that the process takes place. Therefore one of the goals of calculations in QFT is to determine $|M|^2$. As stated earlier, QFT is based upon perturbation theory. This means that we should also consider higher order (quantum) corrections, which can be represented by Feynman diagrams by including loops in the diagram. In figure 3 an example is depicted of such a set of corrections. Diagrams with

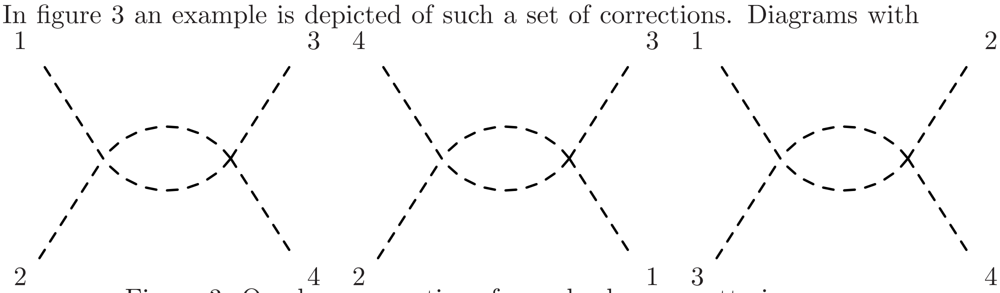

Figure 3: One-loop corrections for scalar boson scattering

one loop correspond with a first order correction, two loops or more correspond with even higher order corrections. Most of the time higher order corrections can be ignored. This will also be the case in this thesis in which up to first order corrections will be considered. These loop corrections are energy dependent and will have a great impact on the high-energy behaviour of the theory.

2.3.1 Renormalization and Coupling

To determine the matrix element M for scalar boson scattering one needs to integrate over all possible loop momenta p. But in a loop all momenta are possible and thus one must integrate to infinity. Instead of taking the upper bound of the loop momentum p as infinite, let's cut off it's components at an arbitrary energy called Λ. This cut-off means that only length scales that are bigger than $\frac{1}{\Lambda}$ are taken into account. It's assumed that down to this length scale the theory is still correct. With this procedure the matrix element belonging to the Feynman diagrams depicted in figures 2 and 3 can be determined. Suppose the center-of-mass energy scale of the process is $\sqrt{s}$, then the matrix element can be written as:

$$M(s) = -\lambda + \frac{\lambda^2}{32\pi^2}\left(3\log\left(\frac{\Lambda^2}{s}\right) + \log\left(\frac{4}{\sin^2(\theta)}\right) + i\pi + 3\right) \tag{15}$$

With λ the quartic coupling constant and θ the center-of-mass scattering angle. From this equation it follows that λ isn't the coupling constant that is measured in experiments[4]. Apparently the quantum corrections are an important part of the effective coupling that is measured with this process. This also means that $|M(s)|^2$ depends on $\log(\Lambda^2)$. This is a problem since it shouldn't be that observations depend on a parameter that can be chosen arbitrarily. Thus the following constraint is made on the derivative of equation (15):

$$\frac{dM}{d\Lambda^2} = 0$$

[4]If it was, the result would be $M = -\lambda$.

This leads to the following equation:

$$0 = \frac{d\lambda}{d\Lambda^2}\left[-1 + \frac{\lambda}{16\pi^2}\left(3\log\left(\frac{\Lambda^2}{s}\right) + \log\left(\frac{4}{\sin^2(\theta)}\right) + i\pi + 3\right)\right] + \frac{3\lambda^2}{32\pi^2}\frac{1}{\Lambda^2} + \mathcal{O}(\lambda^3)$$

This still isn't easy to solve, but at first order in perturbation theory it can be approximated by:

$$-\frac{3\lambda^2}{32\pi^2}\frac{1}{\Lambda^2} \approx -\frac{d\lambda}{d\Lambda^2} \tag{16}$$

Instead of solving this directly, it is easier to make a short detour that will be very useful for making remarks about the final solution.
Let's take a look at another derivative:

$$\frac{d\frac{1}{\lambda}}{d\log\Lambda^2} \tag{17}$$

By rewriting equation (17) it is possible to couple it to equation (16). Doing this gives:

$$\begin{aligned}\frac{d\frac{1}{\lambda}}{d\log\Lambda^2} &= \frac{d\frac{1}{\lambda}}{d\lambda}\frac{d\lambda}{d\log\Lambda^2} \\ &= -\frac{1}{\lambda^2}\left(\frac{1}{\Lambda^2}\frac{d\Lambda^2}{d\lambda}\right)^{-1} \\ &= -\frac{\Lambda^2}{\lambda^2}\frac{d\lambda}{d\Lambda^2} \\ &= -\frac{3}{32\pi^2}\end{aligned} \tag{18}$$

This equation is known as a Renormalization Group Equation (or short: RGE) . This gives us a result that describes the evolution of λ as a function of $\log\Lambda^2$. Solving the previous equation gives the following evolution of λ

$$\frac{1}{\lambda(\Lambda^2)} = \frac{1}{\lambda(s_0)} - \frac{3}{32\pi^2}\log\frac{\Lambda^2}{s_0} \tag{19}$$

Where $\lambda(s_0)$ represents the initial condition of the RGE at the reference energy scale $\sqrt{s_0}$.
There is a dependence on Λ^2, this means that $\lambda(\Lambda^2)$ still isn't the coupling constant that is "observed" in an experiment. Let's introduce a new coupling constant λ_p that is observable at an energy scale $\sqrt{s_0}$. This means it is possible to couple the new coupling constant to equation (15) and find out how $M(s)$ depends on λ_p:

$$\begin{aligned}M(s = s_0) \equiv -\lambda_p &\approx -\lambda + \frac{\lambda^2}{32\pi^2}\left(3\log\left(\frac{\Lambda^2}{s_0}\right) + \log\left(\frac{4}{\sin^2\theta}\right) + i\pi + 3\right) \\ &\longrightarrow 0 = -\lambda + \frac{\lambda^2}{32\pi^2}\left(3\log\left(\frac{\Lambda^2}{s_0}\right) + \log\left(\frac{4}{\sin^2\theta}\right) + i\pi + 3\right) + \lambda_p \\ &\longrightarrow \lambda = \lambda_p + \frac{\lambda_p^2}{32\pi^2}\left(3\log\left(\frac{\Lambda^2}{s_0}\right) + \log\left(\frac{4}{\sin^2\theta}\right) + i\pi + 3\right) + \mathcal{O}(\lambda_p^3)\end{aligned}$$

This new expression was defined at a very specific energy scale $\sqrt{s} = \sqrt{s_0}$ but the goal is to be able to make predictions at any energy scale. Thus let's return to the standard expression for M given by equation 15. We should obtain a matrix element that is independent of Λ^2, just like the observable λ_p:

$$\begin{aligned} M(s) &= -\lambda + \frac{\lambda^2}{32\pi^2}\left(3\log\left(\frac{\Lambda^2}{s_0}\right) + \log\left(\frac{4}{\sin^2\theta}\right) + i\pi + 3\right) + \mathcal{O}(\lambda^3) \\ &= -\lambda_p - \frac{3\lambda_p^2}{32\pi^2}\log\frac{\Lambda^2}{s_0} + \frac{3\lambda_p^2}{32\pi^2}\log\frac{\Lambda^2}{s} + \mathcal{O}(\lambda_p^3) \\ &= -\lambda_p + \frac{3\lambda_p^2}{32\pi^2}\log\frac{s_0}{s} \end{aligned} \tag{20}$$

This is a major improvement. The matrix element is no longer dependent on Λ^2 and only depends on the energy scale at which it is measured. This means that if $M(s)$ is found in an experiment, it is possible to predict its value at a higher energy scale. This process of eliminating λ is called renormalization.
One more thing to notice is the fact that $M(s) \equiv -\lambda_{eff}(s)$ also obeys equation the RGE $-\frac{d\lambda_{eff}(s)}{ds} = -\frac{3\lambda_{eff}^2(s)}{32\pi^2}\frac{1}{s}$ and thus that its evolution as a function of energy is determined by the same equation.

All of this looks very strange, the infinities are still there and were only shifted to a different place. Actually our starting point was incorrect. It was assumed that the parameter λ was the coupling constant that could be measured. But there is no reason to assume that λ was measureable. It was just a parameter of the Lagrangian that was interpreted as the coupling constant. Only after we did higher orders of pertubation theory was it discovered that λ would go to infinity. So a new parameter λ_p was defined in such a way that it represented the physical observed coupling. This in turn gave us the evolution of our theory as a function of the energy scale of the scattering process.
Perturbation theory is defined around the free particle theory in which the interactions are switched off. But in QFT there can't be a free-particle theory, there are always interactions. These are represented by the corrections which in turn created infinities. The starting point that was used for the perturbative expansion was just wrong [11].
After renormalization was applied, we defined new parameters and our theory became finite. The difference is that this time the corrections were a part of the definitions. The corrections were considered from the start and thus the theory became predictive again. Basically the starting point for the perturbative expansion was fixed to create a correct representation of the theory.

For the previous example the process of renormalization worked and produced a predictive theory. However, this isn't always the case, such theories are called non-renormalizable. But even if a system can be renormalized this doesn't solve all the problems. It can even create some new problems. This is the case with the Higgs field as we will see in chapter 3.

2.3.2 Power Counting

The procedure that was done in the previous paragraph was quite long and if the number of diagrams becomes larger it becomes quite a time consuming process. However, there is an easy way to see whether a loop correction diverges, and how it will behave if the cut-off of the energy is taken to infinity. This trick is called *power counting* and uses the fact that Feynman diagrams are only representations of the physics that determine the described processes. The main ingredient for power counting is that every internal line (propagator) in a loop contributes powers in loop-momenta to the matrix element. The powers differ for different spins and are determined by the Feynman rules. For our purpose only the number of powers is relevant and not the precise rules. Therefore the only piece of information needed is that internal spin-0 (scalar) boson propagators give a factor $\frac{1}{p^2}$, and that every fermionic spin-$\frac{1}{2}$ propagator gives a factor $\frac{1}{p}$.

The high energy (cut-off) dependence of a loop integral is given by:

$$\int^{\Lambda} d^4p * p^{-n} \tag{21}$$

In this integral n is the number of negative powers determined via power-counting. Since there are two bosonic propagators in the example in 3 it's easy to determine that $n = 4$ in this case. The next step is to simply cancel out the powers that arise from the integral that we need to perform to obtain the matrix element against the powers that are obtained from power counting. For this specific example it looks like they would cancel each other out completely. But the integral is still there, thus it can't be that all dp terms are canceled (this is the same when using spherical $3D$ coordinates $d\vec{p} \longrightarrow |\vec{p}|^2 d|\vec{p}|$). This gives the following behaviour:

$$\int^{\Lambda} dp\frac{1}{p} \longrightarrow \log\Lambda \tag{22}$$

Just as indicated in paragraph 2.3.1 the evolution of the scalar-boson scattering process is given by a logarithmic dependence on the energy, which presents a problem in the limit where the energy goes to infinity. Thus by using *power counting* we can get a good idea which diagrams diverge and contribute strongly to the energy dependence and which don't.

3 Research

3.1 The High Energy Behaviour of the Higgs Potential

The process of renormalization can be done for the Higgs boson while considering the entire SM. Doing this results in some very different scenarios that may have a great impact on the SM at high energies. Which scenario applies is dependent on the mass of the Higgs boson. The different scenarios give a different evolutionof the physically observable Higgs-boson coupling λ_P as a function of the energy Q. The evolution is roughly given by the RGE:

$$\frac{d\lambda_p(Q)}{d\log Q} \approx \frac{3}{2\pi^2}\left(\lambda_p(Q)^2 + \frac{1}{2}\lambda_p(Q)f_t - \frac{1}{4}f_t^4\right) \tag{23}$$

In this equation the parameter f_t is the coupling constant for the interaction between the top-quark and the Higgs boson. Only this term is mentioned, since it's the heaviest particle in the SM, and therefore has the strongest coupling to the Higgs boson. So by observing how λ_p behaves when only considering f_t, a good approximation is obtained for its high energy behaviour.

The parameter λ_p has a relation to the mass of the Higgs boson via $\lambda = \frac{\mu^2}{v^2} = \frac{M_H^2}{2v^2}$, since the mass of the Higgs boson roughly corresponds to $\frac{\mu}{\sqrt{2}}$. If this is considered it gives three different solutions that depend on what the mass of the Higgs boson actually is.
The first solution corresponds to the case that λ^2 dominates equation 23. This would correnspond to a large mass for the Higgs boson. Thus the other terms can be neglected which would give a differential equation that looks like

$$\frac{d\lambda_p(Q)}{d\log Q} \approx \frac{3}{2\pi^2}\lambda_p^2(Q)$$

This differential equation can be solved giving an evolution that looks like:

$$\lambda_p(Q) = \frac{\lambda_p(s_0)}{1 - \frac{3\lambda_p(s_0)}{4\pi^2}\log\left(\frac{Q^2}{s_0}\right)}$$

The parameter s_0 details an energy scale at which λ_p is known. Thus it serves as a reference point from which λ_p evolves.
This scenario gives rise to a coupling that is going to blow up to infinity. Because there is a value for Q at which $1 - \frac{3\lambda_p(s_0)}{4\pi^2}\log\left(\frac{Q^2}{s_0}\right) = 0$, at this energy scale the coupling would explode. This can't be a proper theory because this process would dominate every process involving the Higgs boson. Clearly this isn't what we want since the goal is to make predictions at every energy scale, including the scale where the coupling goes to infinity. This would mean that there must be new physics to prevent this singularity from occurring.

The second scenario is the opposite of the first. The equation is dominated by the coupling with the top quark. This corresponds to a relatively small mass of the Higgs boson. In this scenario the differential equation is given by:

$$\frac{d\lambda_p(Q)}{d\log Q} \approx -\frac{3}{8\pi^2} f_t^4$$
$$\longrightarrow \lambda_p(Q) = \lambda_p(s_0) - \frac{3}{16\pi^2} f_t^4 \log\left(\frac{Q^2}{s_0}\right)$$

This result is even worse. There's the possibility that the second term becomes larger than the first. This would lead to a negative λ_p. While this doesn't seem like a problem, the implications are enormous. A negative λ_p would give an inverse potential for the Higgs field. This can be seen in figure 4. The second scenario are thus all those cases in which the potential becomes negative.

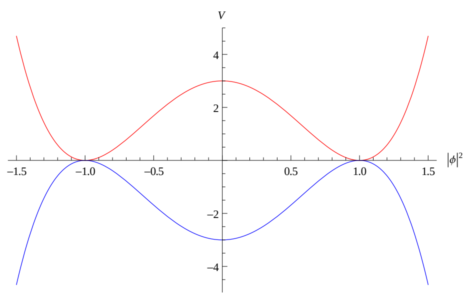

Figure 4: The Higgs potential with a positive and negative λ. The upper line is a Higgs potential for a postive λ, while the lower line is a potential for a negative λ. The values on the axes are arbitrary

The real problem here is the fact that it has become impossible to define a groundstate. The potential goes to negative infinity for $|\phi| \longrightarrow \infty$. It's not possible to find a minimum and thus a particle interpretation cannot be found. This is called vacuum instability and gives problems for the universe in its early energetic stage. Again this means that we expect new physics to prevent λ from becoming negative.

This leaves the last scenario in which no coupling dominates. This scenario is harder to solve. The solution that results from this scenario is very appealing. The Higgs coupling may remain finite and positive, thus the theory remains predictive. This might be the only solution that will leave the SM intact at high energies. Therefore it's the preferred solution from the SM perspective.

The question now is in which domain does the universe reside? Until last summer the answer wasn't known. But with the discovery of the Higgs boson it's now known what scenario applies. The border between the third and second scenario is ~ 130 GeV [6]. This is a problem since the mass of the Higgs boson was discoverd to be 126 ± 0.8 GeV [1]. Apparently the second solution is the valid one, but barely. In order to figure out how rigid this border between scenarios 2 and 3 is, we will try to investigate what the ingredients are that determine if λ becomes negative or not.

3.2 Simplified Model

To see if the problem with the Higgs potential can be better understood, it's convenient to take a look at a simplified model. This model consists of a scalar boson given by the field ϕ', a fermion represented by the Dirac field ψ', a gauge vector field A'_μ and the Higgs potential represented by $V(\phi')$. Interactions between the fermion and scalar boson are also allowed via a Yuwakawa interaction $\propto \bar{\psi}'\phi'\psi'$. This won't be gauge invariant, since the transformation of ψ' and $\bar{\psi}'$ will cancel each other, leaving the transformation of ϕ' with charge $Q = 1$. To solve this, split the fermionic Dirac field in two components ψ'_L and ψ'_R. The transformation of these components will differ and depend on their "charge" Q_L and Q_R as stated in paragraph 2.1. If we take $Q_L + 1 - Q_R = 0$, then a gauge-invariant Yukawa interaction is possible. Doing all this gives a Lagrangian that looks like:

$$\begin{aligned}\mathcal{L} =& i\bar{\psi_R}'(x)\gamma^\mu D^R_\mu \psi'_R(x) + i\bar{\psi_L}'(x)\gamma^\mu D^L_\mu \psi'_L(x) + (D_\mu\phi'(x))^\dagger(D^\mu\phi'(x)) \\ &- V(\phi'(x)) - f_t(\bar{\psi_R}'(x)\phi'(x)\psi'_L(x) + \bar{\psi_L}'(x)\phi'^\dagger(x)\psi'_R(x)) \end{aligned} \tag{24}$$

In this equation γ^μ are the gamma-matrices, D_μ is the derivative defined in equation (7) with the addition that $D^{L,R}_\mu = \partial_\mu + igQ^{L,R}A_\mu$. The Yukawa coupling constant is indicated by f_t, indicating that is is supposed to model the interaction between the top quark and the Higgs boson. The way to shift the field ϕ' was already detailed in section 2.2, where two bosons remained. But only one boson should remain. To see which particle survives, choose a new parametrization for ϕ':

$$\phi' = \frac{1}{\sqrt{2}}(v + H(x))e^{i\frac{w(x)}{v}} \tag{25}$$

In this new parametrization v is the same v as defined in section 2.2. Furthermore for small field values $H(x) \approx \phi_1(x)$ and $w(x) \approx \phi_2(x)$. Now we use the Taylor expansion for the exponent and neglect all orders higher than $w(x)$. Doing this gives the same field we got when shifting the field in section 2.2. The advantage is that $w(x)$ is now a phase in our field parametrization. This means a gauge transformation can be chosen to cancel it, leaving one boson, as was stated earlier:

$$\phi'(x) \longrightarrow \phi(x) = e^{-i\frac{w(x)}{v}}\phi'(x) = \frac{1}{\sqrt{2}}(v + H(x)) \tag{26}$$

But $\phi'(x)$ isn't the only field to change under the gauge transformation. Also $A'_\mu(x)$ changes according to equation (8) and $\psi'_{L,R}(x)$ according to $\psi'_{L,R}(x) \longrightarrow \psi_{L,R}(x) = e^{-iQ_{L,R}\frac{w(x)}{v}}\psi'_{L,R}(x)$. This gives a new transformed vector field $A_\mu(x)$ that has the following form:

$$A_\mu(x) = A'_\mu + \frac{1}{gv}\partial_\mu w(x) \tag{27}$$

This gives a new Lagrangian in terms of the just defined new fields:

$$\begin{aligned}\mathcal{L} =& i\bar{\psi_R}(x)\gamma^\mu D^R_\mu \psi_R(x) + i\bar{\psi_L}(x)\gamma^\mu D^L_\mu \psi_L(x) + (D_\mu\phi(x))^\dagger(D^\mu\phi(x)) \\ &+ \mu^2\phi(x)\phi^\dagger(x) - \lambda(\phi(x)\phi^\dagger(x))^2 - f_t(\bar{\psi_R}(x)\phi(x)\psi_L(x) + \bar{\psi_L}(x)\phi'^\dagger(x)\psi_R(x)) \end{aligned} \tag{28}$$

By inserting the new field $\phi(x)$ the following equation is obtained:

$$\begin{aligned}\mathcal{L} =& i\bar{\psi}_L(x)\gamma^\mu(\partial_\mu + igQ_LA_\mu(x))\psi_L(x) + i\bar{\psi}_R(x)\gamma^\mu(\partial_\mu + igQ_RA_\mu(x))\psi_R(x) \\ &+ ((\partial_\mu + igA_\mu(x))\frac{1}{\sqrt{2}}(H(x)+v))^\dagger((\partial^\mu + igA^\mu(x))\frac{1}{\sqrt{2}}(H(x)+v)) \\ &+ \frac{1}{2}\mu^2(v+H(x))^2 - \frac{1}{4}\lambda(v+H(x))^4 - \frac{1}{\sqrt{2}}f_t(\bar{\psi}(x)(v+H(x))\psi(x)) \quad (29)\end{aligned}$$

This can be written in such a way that it looks less intimidating:

$$\begin{aligned}\mathcal{L} =& i\bar{\psi}(x)\gamma^\mu\partial_\mu\psi(x) + \frac{1}{2}\partial_\mu H(x)\partial^\mu H(x) - \mu^2H(x)^2 - \frac{1}{\sqrt{2}}f_tv\bar{\psi}(x)\psi(x) \\ &+ \frac{1}{4}\mu^2v^2 + \text{int.} \quad (30)\end{aligned}$$

In this compact equation all the mass and kinetic terms were seperated from the interactions[5] which are simply denoted as "int." . These interactions are:

$$\begin{aligned}\text{int.} =& -gQ_L\bar{\psi}_L(x)\gamma^\mu A_\mu(x)\psi_L(x) - gQ_R\bar{\psi}_R(x)\gamma^\mu A_\mu(x)\psi_R(x) - \lambda vH(x)^3 \\ &+ \frac{g^2}{2}A_\mu(x)A^\mu(x)(v+H(x))^2 - \frac{1}{4}\lambda H(x)^4 - \frac{1}{\sqrt{2}}f_tH(x)\bar{\psi}(x)\psi(x)\end{aligned}$$

For our purpose it isn't useful to consider an extra vector field. It was just needed to make a proper gauge transformation. Since this has been done it isn't needed anymore and can be removed from the equations. This can be done by choosing $g << 1$, so that it is possible to neglect any term with g in it. This would make sure that the vector field can be neglected. That is also why we have not implemented any kinetic term for the vector field in the Lagrangian. In this way only the interactions among the scalar bosons and the fermion are left:

$$\text{int.} = -\lambda vH(x)^3 - \frac{1}{4}\lambda H(x)^4 - \frac{1}{\sqrt{2}}f_tH(x)\bar{\psi}(x)\psi(x) \quad (31)$$

These three interactions are all the interactions in our simplified model, which implies that there are only three vertices for the Feynman diagrams.

3.3 Feynman Diagrams and Power Counting

The next step is to determine all diverging contributions in the quantum corrections. This is possible since the vertices that can be used were determined in the previous paragraph. The amount of diagrams we have is increased by the amount of loops that will be considered. For practical purposes only diagrams with one loop will be considered. Besides the number of loops another factor that increases the number of diagrams is the fact that the number of interacting particles isn't limited. It's possible to have an arbitrary number of incoming and outgoing particles. Clearly there is a need to limit the number of particles that can interact, and with it the number of diagrams that are possible.
To do this we limit the number of incoming and outgoing particles to four. This

[5]For those that are paying close attention: yes there is a non-interacting term in the interactions. This is for a reason that will become clear later

reduces the number of diagrams to a manageable magnitude.
These restrictions leave only three groups of diagrams. The first group has one incoming and one outgoing particle. A possible diagram is seen in figure 5.

It's logical that this group is the smallest one since the number of interaction is limited. Furthermore permutations of the particles don't yield any new diagrams. This won't be the case for the other two groups, giving us more diagrams.

Figure 5: A possible diagram with one incoming and one outgoing particle. The solid lines denote the fermions, with the arrow indicating the particle flow. As before, the dashed line denotes the scalar boson.

The second group consists of diagrams with two incoming and one outgoing particles. An example can be seen in figure 6.

There's a difference with the diagram in figure 5. In figure 6 there is a loop of fermionic particles. In contrast to the Higgs boson[6] for fermions there is a difference between the particles and the antiparticles. Thus replacing all fermions with their antiparticles gives a new diagram, displayed in figure 7.

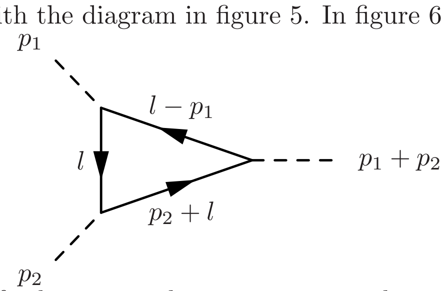

Figure 6: An example of a diagram with two incoming and one outgoing particles

The difference between figure 6 and figure 7 is that the arrows have been

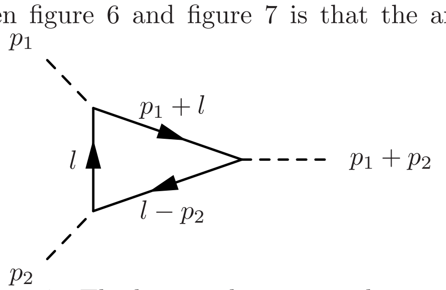

Figure 7: The loop with antiparticles

[6]whose antiparticle is the Higgs boson

reversed. This is the same as interchanging the momenta of the incoming particles. This means that not all different permutations give new diagrams. In some occasions swapping the particles with antiparticles gives the same result as a permutation of momenta. Of course in our simplified model this is only relevant for diagrams that contain fermionic loops.
The last group of diagrams are the diagrams with two incoming and two outgoing particles. Again a diagram is drawn as an example in figure 8.
This group contains the largest number of diagrams since the number of per-

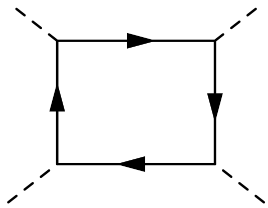

Figure 8: An example with two incoming and outgoing particles

mutations is the largest. For example, the diagram in figure 8 has six different permutations and thus six diagrams of its kind have to be considered for the RGEs.
Now that the groups of diagrams are clear, it's time to look at which diagrams have a divergent high energy (cut-off) dependence. In paragraph 2.3.2 the procedure of power counting was introduced. This will now be used to determine which diagrams converge and which diverge.
An example of a converging diagram is seen in figure 9. With the use of power

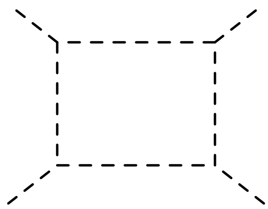

Figure 9: A converging diagram

counting it's easy to see that the diagram in figure 9 has a contribution of 8 inverse powers of energy. This means this particular diagram is highly convergent and doesn't effect the RGE of the Higgs potential. But the diagram in figure 10 is divergent and thus does impact the RGE of the Higgs potential through the coupling λ.
Again with the use of power counting its impact can be determined. For the diagram in figure 10 the contribution is quadratically divergent. This diagram is highly divergent. This means that it's expected that this diagram will greatly impact the evolution of λ as a function of energy.
An overview of all possible diagrams with the number of permutations and an indication whether they are divergent or convergent can be seen in the Appendix.

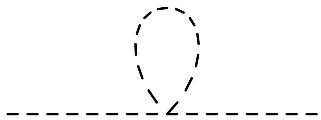

Figure 10: A diverging diagram

Before going to the RGE of the Higgs potential, let's return to the problem of the unlimited number of Feynman diagrams. This was solved by limiting the number of incoming and outgoing particles. But was information lost in this process?
If information was lost this would be disastrous. Since there is an infinite number of diagrams it's easy to imagine that a great deal of information was neglected by limiting the number of diagrams. Let's look at a new diagram of three incoming and two outgoing particles that was not considered before. By this we mean a diagram that does not contain a loop diagram with less than 5 particles as building blocks. Such a diagram is called 1-particle irreducible. First let's take a look at the most likely candidate for a diverging diagram. Since fermions have a $\frac{1}{p}$ dependence while bosons have a $\frac{1}{p^2}$ dependence, it's logical to expect the most diverging diagram to consist fully of fermionic lines. The corresponding diagram can be seen in figure 11
But with power counting it can easily be seen that this diagram is converging.

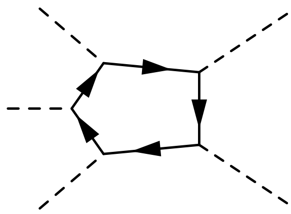

Figure 11: A Feynman diagram with 3 incoming and 2 outgoing particles

As was previously said this was expected to be the diagram with the greatest chance of being divergent. Thus it can be expected that all 1-particle irreducible diagrams with 5 particles are convergent, and they are. Obviously the same holds for more than 5 particles. Thus the conclusion can be drawn that 1-particle irreducible diagrams with more than four particles are all convergent. This conclusion also means that no information was lost for the RGE by limiting the number of particles.

With the diagrams determined, it's now possible to calculate the renormalization group equations that are needed to determine the evolution of the parameters in the Higgs potential. The deriviation of this equation will not be shown in this thesis, only the outcome will be noted and used in the next section.

3.4 Renormalizing the Higgs Potential

By using the procedure that was explained in paragraph 2.3 and the diagrams that are listed in the abstract, it's possible to determine the RGE for the parameter λ:

$$\frac{d\lambda}{d\log Q} = \frac{9}{8}\frac{\lambda^2}{\pi^2} + \frac{\lambda f_t^2}{4\pi^2} - \frac{f_t^4}{8\pi^2} \tag{32}$$

The evolution of λ is now determined by the combination of two constraints. Firstly the relative size of f_t and secondly the value of λ_s, the value of λ at energy scale $\sqrt{s_0}$. Changing either value gives a different evolution. In figure 12 the evolution of λ is plotted while the value of λ_s is changed and f_t remains constant.

In figure 12 it's clearly seen that a larger value for λ_s implies a possible

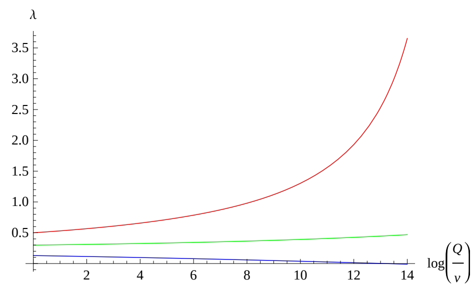

Figure 12: The evolution of λ for 3 different values of λ_s. The blue line is $\lambda_s = 0.13$, the green line $\lambda_s = 0.3$ and the red line $\lambda_s = 0.5$. Futhermore f_t is kept constant at $f_t \approx 1$

growth of λ. This corresponds to the observations made in paragraph 3.1. If the λ term dominates, this would lead to a positive evolution. If the range of the energy is large enough, a singularity is expected to appear. This can already be seen from the red line.
In contrast, a small value of λ_s gives a negative evolution. Again this matches our observations from paragraph 3.1. Thus it can be said that changing the value of λ_s has a clear impact on the evolution of λ. But f_t also has an impact as can be seen in figure 13.
In contrast to a variation of λ_s a larger f_t corresponds to a faster decline of λ. This isn't surprising since it's possible to use the same reasoning we used earlier. The observations in paragraph 3.1 told us that for increasing f_t the evolution will go through zero at a decreasing energy scale.
With the effects of f_t and λ_s now known, all that is needed are the correct values to determine the evolution of λ. However there is one more bump in the road, and it's quite large. In paragraph 2.3.1 we treated f_t as a constant, i.e. we had only one RGE. But now there are in fact two RGEs, the second one corresponding to f_t:

$$\frac{df_t}{d\log Q} = \frac{5f_t^3}{32\pi^2} \tag{33}$$

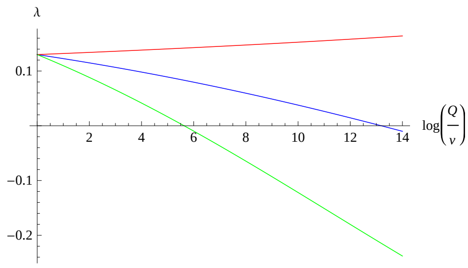

Figure 13: The evolution of λ for 3 different values of f_t. The blue line is $f_t = 1$, the green line $f_t = 1.2$ and the red line $f_t \approx 0$. This time λ_s is kept constant at $\lambda_s = 0.13$

This means that the previous analysis is incomplete, since the evolution of f_t needs to be taken into account. But the evolution is still governed by λ_s and now also the initial condition for f_t called $f_{t,0}$ which plays the same role as the constant f_t.
To get a complete picture of the evolution of λ both RGEs need to be combined, since the evolution of f_t will change the evolution of λ. Instead of computing the result analytically it can also be solved numerically by using Mathematica [12]. Before this can be done, the parameters λ_s and $f_{t,0}$ need to be determined. Luckily these values are easily determined via the masses. In equation (30) the lowest prder connection between the parameters λ_s, $f_{t,0}$ and the masses of the Higgs boson and the top quark can be seen:

$$M_H^2 = 2\lambda_s v^2 \tag{34}$$

$$m_t = \frac{1}{\sqrt{2}} v f_{t,0} \tag{35}$$

This leads to the following values of λ_s and $f_{t,0}$.

$$\lambda_s = \frac{1}{2}\frac{M_H}{v^2} \approx 0.13 \tag{36}$$

$$f_{t,0} = \sqrt{2}\frac{m_t}{v} \approx 0.994 \tag{37}$$

Here v is the expectation value of the groundstate with a value of $v = 246$ GeV, M_H is the mass of the Higgs boson with a value of $M_H = 125.3$GeV and m_t is the mass of the top quark with a value of $m_t = 172.9$ GeV.
By inserting these values into the computer code the coupled RGEs can be solved nummerically. Doing this results in the following evolution.
While both lines go through zero the difference is quite big. When only the λ-RGE is considered, λ becomes negative for a relatively large energy. However with the combined RGEs λ declines much faster. This results in a negative λ well before the Planck scale, which is situated around $\log \frac{Q}{v} = 16$. The Planck scale is a scale where new physics is expected, since gravity plays a significant role at such energies. Therefore, if the SM can be extended to the Planck scale that might be an indication that there is no new physics before this scale.

This analysis isn't complete of course. There are other contributions that are

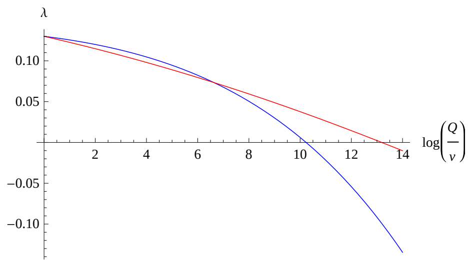

Figure 14: The evolution of λ. The brown line is the evolution of λ without the RGE of f_t. The blue line includes the RGE of f_t

ignored here, like the ones corresponding to the other particles in the SM. What are the expected consequences of these contributions?
One could imagine that the extra particles in the SM might save the Higgs potential but unfortunately most of these contributions are negligible in comparison with the top quark contribution.
However there are some possiblities to tweak the evolution and there is one sector of the SM that can't be ignored.

3.5 Tweaking the Evolution

In the previous paragraph it was shown that the simplified model exhibited the same general evolution of λ as the complete SM. The next step is to try and change this evolution without the introduction of new interactions or new particles. So what can be changed? One of the logical scenarios is to lose one of the SM constraints to gain more freedom in choosing our solution. For this thesis a model was considered in which equation (11) was allowed to become energy dependent. In terms of the parameters v and λ it means that they may evolve independently of each other. This would give a third RGE and thus possibly new solutions.
The renormalization of v has a surprising effect. By renormalization the value of v is shifted, but as a result of this shift new terms arise in the RGE that shift the renormalized value of v back to it's original value before renormalization. The RGE of v apparently has no new information, even if v is allowed to change, its renormalized value will remain constant and equation (11) will hold [9]. The value of v was an indication of the position of the minimum of the potential. That it remains constant under renormalization means that the minimum won't change position if the energy scale is increased.

Another possibility is that the wrong values were taken for the masses of either the Higgs boson or the top quark. These particles have known error margins on their measured masses and it's possible to study the change in the evolution within these margins.
First let's insert the error margins for the Higgs boson. As seen in figure 15 the impact on the evolution can barely be seen. Mostly the starting point is changed but the general evolution stays the same. The next thing that can be done is changing the evolution of f_t by varying $f_{t,0}$ within the measurement

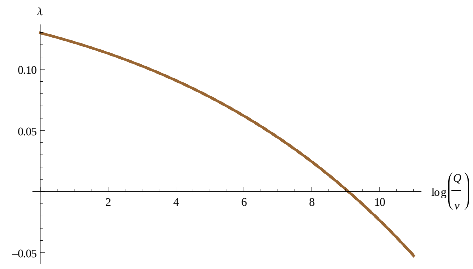

Figure 15: The evolution of λ for different values of M_H. The thick line is the evolution of λ for the Higgs boson mass without measurement error and the dashed lines represent the error margins

error margins. Again the effect isn't significant in figure 16. The energy at

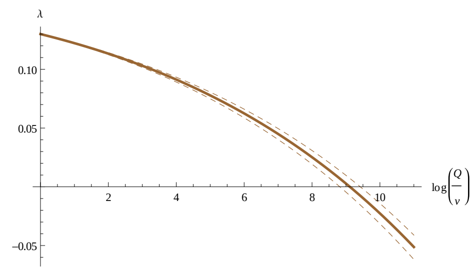

Figure 16: The evolution of λ for different values of m_t. The thick line is the evolution of λ for the top quark mass without measurement error. Again the dashed lines represent the error margins

which λ becomes negative is of the same order of magnitude as in figure 15. The difference is that the evolution is now clearly impacted after the starting point. Thus maybe by combining these two different evolutions an effect can be found. In figure 17 the combined effect of the error margins can be seen. The error margins have been combined to be the most effective. This means that the largest value of M_H is combined with the smallest value of m_t and vice versa. From the earlier analysis in paragraph 3.1 it's expected that the former is the most likely candidate for keeping λ positive at higher energies. Unfortunately even this optimal combination becomes negative well before the Planck scale. This is because the effect of the error margins on the mass of the Higgs boson are so small. The combined evolution looks like the evolution in figure 17 and can barely be distinguished from the evolution without the error margins in the Higgs mass as seen in figure 16. It should be noted that this analysis isn't a correct statistical analysis. Its only goal is to see what the elbow room is for changing the evolution within the simplified model.

Before dismissing all chance of keeping λ positive within the SM, let's look for more options to try. The masses that we inserted in the previous analysis where the measured masses. But these masses are measured from the particle resonances. Only at lowest order are these masses related to the coupling λ and

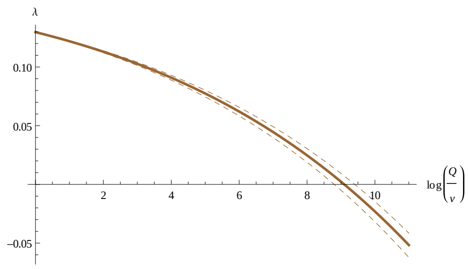

Figure 17: The evolution of λ for different values of M_H and m_t. The thick line is the evolution of λ for the masses without measurement errors. The lower dashed line indicates the combination of the largest m_t value with the smallest M_H value within the error margins. The upper dashed line combines the largest M_H value and smallest m_t value.

f_t according to equations 34 and 35. But the whole point of the RGEs was to include the higher order correction into the definitions of the couplings. We shouldn't look at the masses but at the couplings. These can be calculated from the masses including higher order corrections. The new initial couplings are $\lambda_s = 0.12577 \pm 0.0014$ [5] and $f_{t,0} = 0.937 \pm 0.016$ [2]. The difference between these values and the values used earlier is quite large. These new parameters will be called the running mass input. With these new parameters a new plot can be made. From figure 18 it's clear that the use of the running mass input

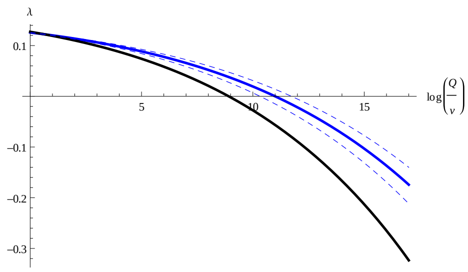

Figure 18: The evolution with the running mass input. The black thick line is the standard fit with the previous values. Again the extreme error margins are denoted by the dashed lines.

has a huge impact on the evolution. Previously the point where λ became zero was around 10^{11} GeV, now this point is 10^{13} GeV.
Already we have seen quite an impact from including the evolution of extra parameters in this simplified model. The inclusion of the evolution of f_t had a great effect and after using the correct input values the evolution changed again. This raises the question whether the Planck scale can be reached by expanding the model with other relevant interactions. The most likely candidate is the strong interaction since it will dominate in the beginning of the evolution.

3.6 Adding the Strong Interactions

Up until now only the interactions between the Higgs boson and the top quark have been considered. But at the start of the evolution, the coupling of the strong interactions is the largest. This means that for a better model one should also consider the strong interactions. This will introduce new diagrams that will alter the RGE of both λ and f_t. Furthermore it will introduce a new coupling which will be called g_s. The derivation of the new RGE will not be shown here and was determined with the help of [4].
The new RGEs are:

$$\frac{d\lambda}{d\log Q} = \frac{9}{8}\frac{\lambda^2}{\pi^2} + \frac{N_c f_t^2 \lambda}{4\pi^2} - \frac{N_c f_t^4}{8\pi^2} \tag{38}$$

$$\frac{df_t}{d\log Q} = \frac{(2N_c+3)\, f_t^3}{32\pi^2} - \frac{3 f_t g_s^2 \left(\frac{N_c^2-1}{2N_c}\right)}{8\pi^2} \tag{39}$$

$$\frac{dg_s}{d\log Q} = \frac{g_s^3}{8\pi^2}\left(-\frac{11}{6}N_c + 2\right) \tag{40}$$

In these equations N_c is the number of colours. In the case of the SM this means $N_c = 3$. If $N_c = 1$ is taken this yields our previous model. It can be seen that for λ only some factors have changed but the overall equation has stayed the same. This can't be said for f_t for which an extra term appeared. This is to be expected since the strong interactions will only "talk" to the Higgs boson via the massive quarks, in this case the top quark. Having learned from past mistakes g_s is immediately taken as a running coupling.
The largest effect is observed for the evolution of f_t, as can be seen in figure 19. The blue line in figure 19 represents the previous model while the black line is

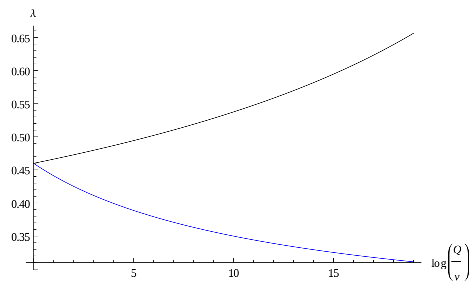

Figure 19: The evolution of f_t with and without the strong interactions. The black line includes the strong interactions while the blue line doesn't

the new model with the strong interactions. The difference is quite clear. Where f_t used to grow as a function of energy, now it decreases. This is due to the effect of g_s on the RGE of f_t . However, g_s itself becomes smaller with energy. Thus one could conclude that in the high energy limit g_s has a small effect on f_t. But the crucial part is that at the start of the evolution f_t is dominated by g_s and thus decreases. At a higher energy f_t is smaller in such a way that g_s still dominates. As can be seen in figure 20 the shape of the evolution for λ is changed radically from the evolution in figure 17. Another effect of introducing the strong interaction is an increased sensitivity to the variation in M_H and m_t

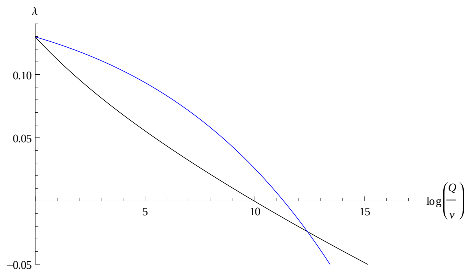

Figure 20: The evolution of λ with and without the strong interactions. The black line includes the strong interactions while the blue line doesn't

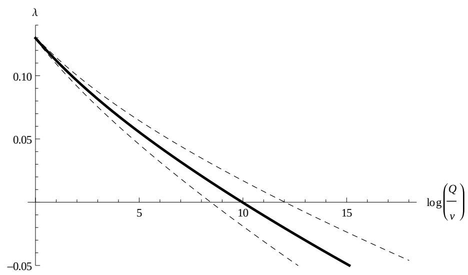

Figure 21: The error margins on the evolution of λ, which are again represented by the dashed lines

as can be seen in figure 21.
To truly see the difference let's compare the model with the strong interactions to the model without the strong interactions. It can be seen from figure 22 that the spread in the evolution trajectories is much greater when the strong interactions are activated. This can be explained by the greater sensitivity to the measurement error margins. Fortunately the old crossing area[7] is still contained within the new crossing area. The main effect is a lowering of the lower crossing scale[8]. Thus overall the expected energy at which λ becomes zero has decreased.
Before drawing conclusions, let's look at the evolution of the other couplings in the SM. Since they all evolve following a different trajectory.
The different evolutions of the couplings are shown in figure 23. It can be clearly seen that the strong coupling dominates at low energy scales. Furthermore we indeed observe that f_t (called y_t in reference []Degrassi) is suppressed by g_s. At high energies the strong interaction doesn't dominate anymore. Instead the electromagnetic coupling takes over while the weak interactions also get more noticeable. It's therefore safe to say that for a better picture a complete analysis of the SM RGEs must be made before any definitive conclusions can be drawn about the evolution of λ.

[7]the area in which λ goes through zero
[8]The energy at which the crossing area begins

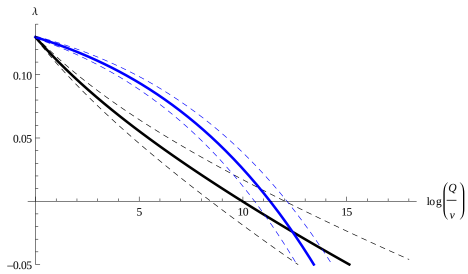

Figure 22: Comparison between both models. The error margins are again represented by the dashed lines

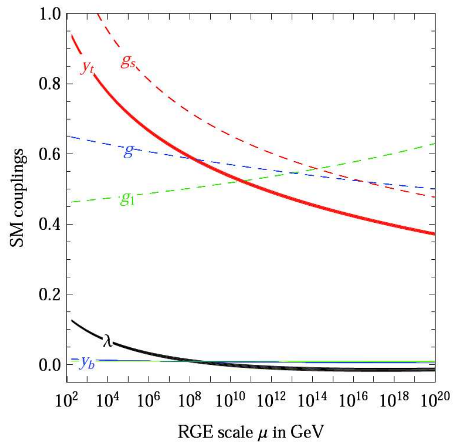

Figure 23: The evolution of the couplings in the SM taken from reference [5]

4 Conclusion

By using a simplified model with only the top quark, Higgs boson and an interaction between these two particles, it was determined that the evolution of the Higgs potential parameter λ can't be changed radically within the SM. If we drop the constant-v restriction on the evolution, the theory still gives a constant renormalized v independent of the energy. This means all parameters have a defined evolution since μ is coupled to λ via the constant v. It should be noted that the use of the correct input values is paramount since these values do have a noticeable effect on the evolution. The only large impact on the evolution is obtained by adding a new coupling. This was performed for the strong interactions, which impacted the model severely. From this reasoning it seems logical to make a complete analysis of the evolution of λ within the SM. Especially since the strong interactions don't dominate in the high energy limit, further study is required. Since the electromagnetic interaction becomes the dominant interaction at higher energies, it is important to include the RGE of this interaction in the analysis.

With the use of the correct values for the input parameters and the inclusion

of the strong interactions, it can be concluded that new physics is expected before 10^{12} GeV, well before the Planck scale. The value found in the literature is around 10^{10} GeV [5]. The difference can be explained by the fact that in reference [5] higher order corrections are used, as well as more sophisticated programming.
The fact that λ goes to zero isn't a problem, some theories of inflation after the Big Bang even need a λ close to zero. However, in all theories a λ that becomes negative is a big problem. At the moment there are several new theories like supersymmetry or heavy righthanded neutrinos that prevent this from happening [5, 6]. These theories are currently being researched at the Large hadron Collider in Geneva. By improving the analysis of the evolution of the Higgs potential in the SM, the energy scale at which such new physics theories should appear can be better predicted.

References

[1] Georges Aad et al. Observation of a new particle in the search for the Standard Model Higgs boson with the ATLAS detector at the LHC. *Phys.Lett.*, B716:1–29, 2012.

[2] S. Alekhin, A. Djouadi, and S. Moch. The top quark and Higgs boson masses and the stability of the electroweak vacuum. *Phys.Lett.*, B716:214–219, 2012.

[3] Wim Beenakker. Lecture notes: Quantum field theory, standard model crash course, 2012.

[4] K.G. Chetyrkin and M.F. Zoller. Three-loop β-functions for top-Yukawa and the Higgs self-interaction in the Standard Model. *JHEP*, 1206:033, 2012.

[5] G. Degrassi et al. Higgs mass and vacuum stability in the Standard Model at NNLO. *JHEP*, 1208:098, 2012.

[6] J. Elias-Miro et al. Higgs mass implications on the stability of the electroweak vacuum. *Phys.Lett.*, B709:222–228, 2012.

[7] J. Ellis, J.R. Espinosa, G.F. Giudice, A. Hoecker, and A. Riotto. The Probable Fate of the Standard Model. *Phys.Lett.*, B679:369–375, 2009.

[8] Jacek Dobaczewski. Non-Linear σ Model. http://www.fuw.edu.pl/ dobaczew/maub-42w/node12.html.

[9] Jins de Jong. Hybrid renormalization and the β-functions of the real scalar Higgs lagrangians from the scalar spectral action. Masterthesis. www.ru.nl/thef/research/master_theses .

[10] Pim van Oirschot. "Weyl die theorie der Eichinvarianz sehr schön ist" en fysische argumenten voor het ijkprincipe. Bachelorthesis. www.ru.nl/thef/research/bachelor_theses .

[11] Wim Beenakker. Lecture notes: Quantum field theory, 2012.

[12] Inc. Wolfram Research. Mathematica edition: Version 9.0.

5 Appendix

In this table all possible diagrams in the simplified model are listed. The number of permutations denotes the number of diagrams possible for this diagram. The column with Powercounting gives the amount of negative powers each diagram provides. The final column states whether the diagram is divergent and, if that is the case, what kind of divergence it has.

Diagram	Number of Permutations	Powercounting	Divergence
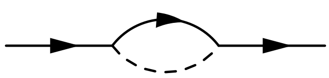	1	3	Logarithmic
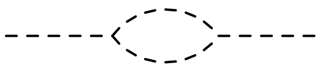	1	4	Logarithmic
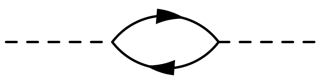	1	2	Quadratic
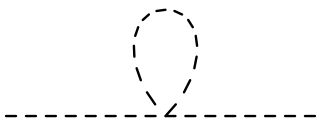	1	2	Quadratic
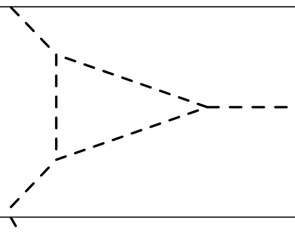	1	6	Convergent
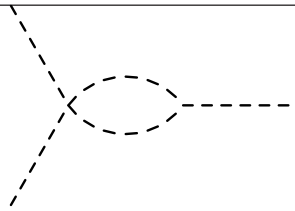	3	4	Logarithmic

Diagram	Number of Permutations	Powercounting	Divergence
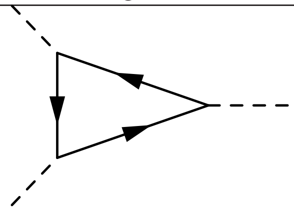	2	3	Logarithmic
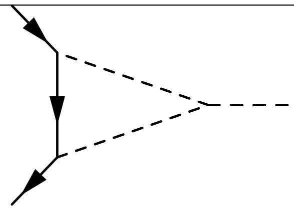	1	5	Convergent
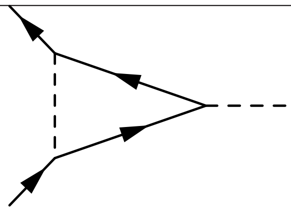	1	4	Logarithmic
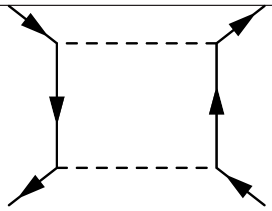	4	6	Convergent
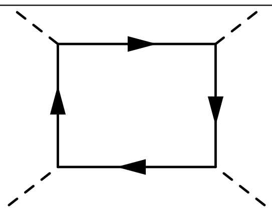	6	4	Logarithmic
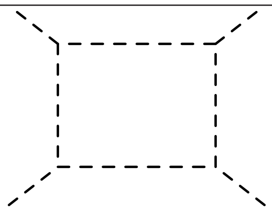	3	8	Convergent
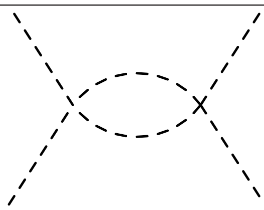	3	4	Logarithmic

Diagram	Number of Permutations	Powercounting	Divergence
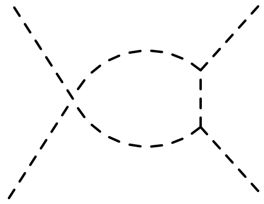	6	6	Convergent
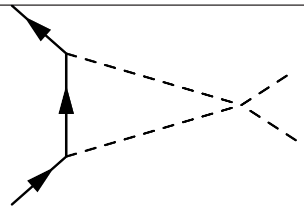	1	5	Convergent
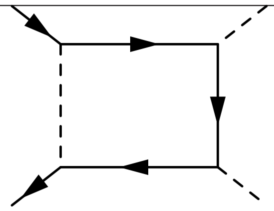	2	5	Convergent
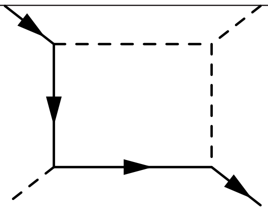	2	6	Convergent
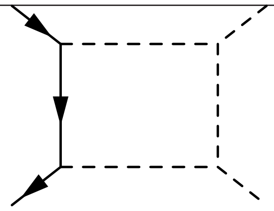	2	7	Convergent